Advanced Design of Phased Array Beam-forming Networks

R. A. Speciale
Research & Development Inc, USA

Abstract—Recent fundamental results [1] in the theory of linear, multi-port networks enable cost-effective, higher-reliability designs for electronically-steered phased arrays. The referenced paper documents and proves that, by including a properly designed beam-forming network, it becomes possible to feed an array and steer its beam, using a much reduced number of expensive and critical phase- and amplitude-controlled sources, while at the same time completely eliminating the adverse effects of element coupling. Those new results are based on a generalization of the classical concepts of *scalar* image impedance, and of *scalar* image-transfer function for two-port networks, to the new concepts of multidimensional image-impedance *matrix*, and of multidimensional image-transfer function *matrix* for linear multi-port networks.

1. The Price of Performance

Electronically-steered phased arrays provide unsurpassed agility and high angular resolution in beam-pointing, and the capability of adaptive, multifunction performance. Such highly desirable features are however only attained at the price of high cost, extreme complexity, and limited reliability. Indeed, electronically-steered phased arrays are almost always designed as active-aperture system, that include a large number of semiconductor devices and beamsteering control-elements, embedded in the physical array structure, and closely connected with all the array radiating elements. The phased arrays used in radar systems use transmit/receive modules (T/R), essentially tiny radar, each nested behind a radiating element, in a half-wavelength square section of the total array aperture. Because of the well-known low power-efficiency of semiconductors, a large heat-flux is developed locally, thus generating a complex cooling problem. Finally, notwithstanding technology advances the semiconductor devices and beam-steering control-elements still are the most expensive components of electronically-steered phased array, and cost-effective designs would only be attained by reducing their total number. Those cost and reliability advantages are however only attainable if the structure of the beam-forming network used establishes a pattern of *synergistic connectivity*, where *each* controlled source simultaneously feeds *all* the array elements, and *each* array element is simultaneously fed by *all* the sources (Figures 1 and 2).

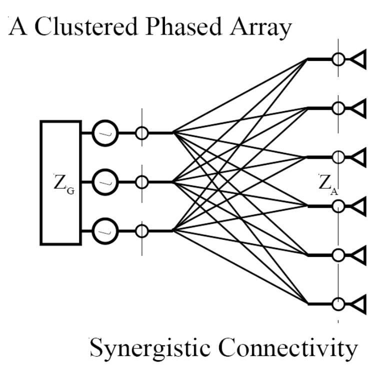

Figure 1: A clustered phased array providing synergistic connectivity.

$$\sum_{1}^{N} \vec{E}_{ej} = \sum_{1}^{n} \vec{E}_{si}$$

$\vec{E}_{ej}$ = **Aperture Field Generated by Element** j | $\vec{E}_{si}$ = **Aperture Field Generated by Source** i

Figure 2: The aperture field is a superposition of components.

2. Non-symmetric Beam-forming Network

Such cost and complexity reductions could only be feasible by including a non-symmetric, multiport beam-forming network between the reduced number of active devices, and the much larger number of array radiating elements. Such beam-forming network would necessarily be non-symmetric, because of including an $\boldsymbol{n}$-port interface on the side of the active devices, and an $\boldsymbol{N}$-port interface on the side of the array radiating elements, with $\boldsymbol{n} < \boldsymbol{N}$ (Figures 3 and 4). The use of a reduced number of beam-steering control-elements appears possible, by considering that current active apertures have the capability of creating a very large number of completely superfluous aperture distributions, that do not generate any practical radiation pattern. Also, the angular resolution of beam-steering could be without penalty reduced, by steering the beam in increments being only a fraction of the –3 dB beam-width.

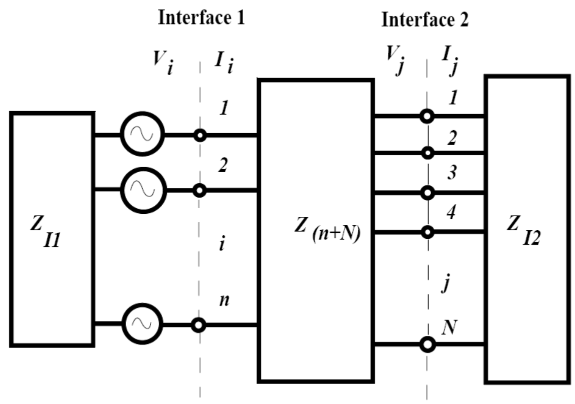

Figure 3: Unconditional, bilateral image-impedance match: forward-wave, n-phase excitation, with arbitrary wave amplitudes and phases.

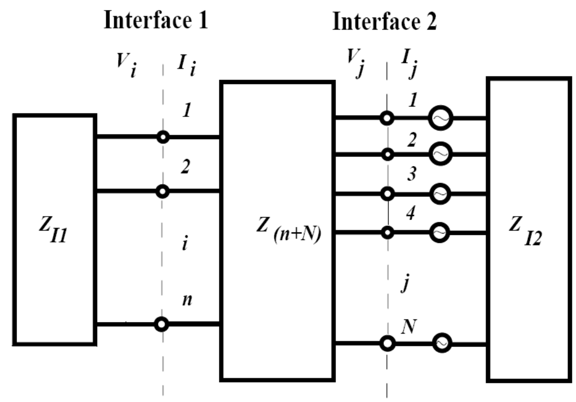

Figure 4: Unconditional, bilateral image-impedance match: backward-wave, N-phase excitation, with arbitrary wave amplitudes and phases.

3. Recent Theoretical Results

The referenced, recent fundamental results [1] in the theory of multi-port networks have been attained by introducing a generalization of the classical concept of scalar image-impedance of two-port networks, to that of image-impedance *matrices* for multiport networks. Similarly, the classical concept of scalar image-transfer function of two-port networks, has been generalized to that of image-transfer function *matrices* for multiport networks. These generalizations have made possible the design of non-symmetric beam-forming networks, that are simultaneously impedance-matched to the external environment at both interfaces, while having prescribed two-way transfer functions between two interfaces with different number of ports ($\boldsymbol{n} < \boldsymbol{N}$).

4. Image Impedance Matrices

The first fundamental new result expresses the $\boldsymbol{n} \times \boldsymbol{n}$ image-impedance matrix $\boldsymbol{Z}_{I1}$ for the $\boldsymbol{n}$-port interface-1, and the $\boldsymbol{N} \times \boldsymbol{N}$ image-impedance matrix $\boldsymbol{Z}_{I2}$ for the $\boldsymbol{N}$ -port interface-2, as functions of the four different-size blocks $\boldsymbol{Z}_i$ of the $(\boldsymbol{n}+\boldsymbol{N}) \times (\boldsymbol{n}+\boldsymbol{N})$ impedance matrix of a non-symmetric, multi-port network:

$$Z_{I1} = (I_n - Z_2 \cdot Z_4^{-1} \cdot Z_3 \cdot Z_1^{-1})^{1/2} \cdot Z_1 = (I_n - P_n)^{1/2} \cdot Z_1 \tag{1}$$

$$Z_{I2} = (I_N - Z_3 \cdot Z_1^{-1} \cdot Z_2 \cdot Z_4^{-1})^{1/2} \cdot Z_4 = (I_N - P_N)^{1/2} \cdot Z_4 \tag{2}$$

where the $\boldsymbol{n} \times \boldsymbol{n}$ matrix product $\boldsymbol{P}_n$, and the $\boldsymbol{N} \times \boldsymbol{N}$ matrix product $\boldsymbol{P}_N$ are given by:

$$P_n = M_n \cdot M_N = Z_2 \cdot Z_4^{-1} \cdot Z_3 \cdot Z_1^{-1} = M_{Pn} \cdot \Lambda_{Pn} \cdot M_{Pn}^{-1} \tag{3}$$

$$P_N = M_N \cdot M_n = Z_3 \cdot Z_1^{-1} \cdot Z_2 \cdot Z_4^{-1} = M_{PN} \cdot \Lambda_{PN} \cdot M_{PN}^{-1} \tag{4}$$

The partial matrix-products $\boldsymbol{M}_n$ and $\boldsymbol{M}_N$ in the expressions Eqs. (3) and (4) are defined as:

$$M_n = Z_2 \cdot Z_4^{-1} \tag{5}$$

$$M_N = Z_3 \cdot Z_1^{-1} \tag{6}$$

and the matrix products $\boldsymbol{P}_n$, and $\boldsymbol{P}_N$ are mutually related by the expression:

$$P_N \cdot (M_N \cdot M_{Pn}) = M_N \cdot (M_n \cdot M_N) \cdot M_{Pn} = M_N \cdot P_n \cdot M_{Pn} = (M_N \cdot M_{Pn}) \cdot \Lambda_{Pn} \tag{7}$$

By connecting external load-networks with internal impedance matrices $\boldsymbol{Z}_{L1} = \boldsymbol{Z}_{I1}$ and $\boldsymbol{Z}_{L2} = \boldsymbol{Z}_{I2}$ to the two interfaces, the two image-impedance matrices will transform to each other through the non-symmetric network:

$$Z_{I1} = Z_1 - Z_2 \cdot (Z_4 + Z_{I2})^{-1} \cdot Z_3 \tag{8}$$
$$Z_{I2} = Z_4 - Z_3 \cdot (Z_1 + Z_{I1})^{-1} \cdot Z_2 \tag{9}$$

5. The Block-traceless Scattering Matrix

Because of the bilateral impedance match so attained, the $(\boldsymbol{n} + \boldsymbol{N}) \times (\boldsymbol{n} + \boldsymbol{N})$ scattering matrix $\boldsymbol{S}$ of the nonsymmetric network becomes *block-traceless*, with only the two rectangular blocks $\boldsymbol{S}_2$ and $\boldsymbol{S}_3$ being non-zero:

$$S = \begin{vmatrix} 0 & S_2 \\ S_3 & 0 \end{vmatrix} \tag{10}$$

$$S_2 = Z_2 \cdot Z_4^{-1} \cdot \left[I_N + (I_N - Z_3 \cdot Z_1^{-1} \cdot Z_2 \cdot Z_4^{-1})^{1/2} \right]^{-1} \tag{11}$$

$$S_3 = Z_3 \cdot Z_1^{-1} \cdot \left[I_n + (I_n - Z_2 \cdot Z_4^{-1} \cdot Z_3 \cdot Z_1^{-1})^{1/2} \right]^{-1} \tag{12}$$

6. Modal and Spectral Analysis

Two other fundamental new results express the modal matrix $\boldsymbol{M}_S$, and the spectral matrix $\boldsymbol{\Lambda}_S$ of the *autonormalized* (normalized to the matrices $\boldsymbol{Z}_{I1}$ and $\boldsymbol{Z}_{I2}$), *block-traceless* $(\boldsymbol{n}+\boldsymbol{N}) \times (\boldsymbol{n}+\boldsymbol{N})$ scattering matrix $\boldsymbol{S}$ as:

$$M_S = \begin{vmatrix} M_1 & M_2 \\ M_3 & M_4 \end{vmatrix} \tag{13}$$

$$\Lambda_S = \begin{vmatrix} \Lambda_1 & 0 \\ 0 & \Lambda_4 \end{vmatrix} \tag{14}$$

The modal matrix $\boldsymbol{M}_S$ has two square diagonal blocks $\boldsymbol{M}_1$ of size $\boldsymbol{n} \times \boldsymbol{n}$, and $\boldsymbol{M}_4$ of size $\boldsymbol{N} \times \boldsymbol{N}$, and two rectangular blocks $\boldsymbol{M}_2$ of size $\boldsymbol{n} \times \boldsymbol{N}$, and $\boldsymbol{M}_3$ of size $\boldsymbol{N} \times \boldsymbol{n}$, while the blocks $\boldsymbol{\Lambda_1}$ and $\boldsymbol{\Lambda_2}$ are $\boldsymbol{n} \times \boldsymbol{n}$, and $\boldsymbol{N} \times \boldsymbol{N}$:

$$M_1 = M_{Pn} \tag{15}$$
$$M_2 = -P_n^{-1/2} \cdot Z_2 \cdot Z_4^{-1} \cdot M_{PN} \tag{16}$$
$$M_3 = Z_3 \cdot Z_1^{-1} \cdot M_{Pn} \cdot \Lambda_{Pn}^{-1/2} \tag{17}$$
$$M_4 = M_{PN} \tag{18}$$
$$\Lambda_1 = \Lambda_{Pn}^{1/2} \cdot \left[I_n + (I_n - \Lambda_{Pn})^{1/2} \right]^{-1} = Diag(e^{-\gamma_n}) \tag{19}$$
$$\Lambda_4 = -\Lambda_{PN}^{1/2} \cdot \left[I_N + (I_N - \Lambda_{PN})^{1/2} \right]^{-1} = Diag(e^{-\gamma_N}) \tag{20}$$

Most remarkably, the block $\boldsymbol{\Lambda}_4$ includes $\boldsymbol{N} - \boldsymbol{n}$ identically-zero eigenvalues, that correspond to the $\boldsymbol{N} - \boldsymbol{n}$ identically-zero eigenvalues of the spectral matrix $\boldsymbol{\Lambda}_{PN}$ of the matrix $\boldsymbol{P}_N$, while the remaining $\boldsymbol{n}$ eigenvalues are equal to those in block $\boldsymbol{\Lambda}_1$, save for a sign change. The $2\boldsymbol{n}$ non-zero eigenvalues in the spectral matrix $\boldsymbol{\Lambda}_S$, and the corresponding eigenvectors, identify the two sets of $\boldsymbol{n}$ *forward*, and $\boldsymbol{n}$ *backward, natural transmission modes* of any given non-symmetric beam-forming network, while the $\boldsymbol{N} - \boldsymbol{n}$ eigenvectors, that correspond to the zero-eigenvalues in block $\boldsymbol{\Lambda}_4$, span the *null-space* of the $\boldsymbol{n} \times \boldsymbol{N}$ block $\boldsymbol{S}_2$, and identify the *natural cut-off* modes of the network. These are the $\boldsymbol{N} - \boldsymbol{n}$ voltage-wave $\boldsymbol{a}_j$ vectors of the $\boldsymbol{N}$-port interface-2, for which the *received* $b_i = S_2 \cdot a_j$ vectors of the $\boldsymbol{n}$-port interface-1 are all identically zero.

7. The Required Impedance Matrix

The final referenced fundamental result expresses the two square blocks $\boldsymbol{Z}_1$ of size $\boldsymbol{n} \times \boldsymbol{n}$, $\boldsymbol{Z}_4$ of size $\boldsymbol{N} \times \boldsymbol{N}$, and the two rectangular blocks $\boldsymbol{Z}_2$ of size $\boldsymbol{n} \times \boldsymbol{N}$, and $\boldsymbol{Z}_3$ of size $\boldsymbol{N} \times \boldsymbol{n}$, as functions of the two required imageimpedance matrices $\boldsymbol{Z}_{I1}$ and $\boldsymbol{Z}_{I2}$, and of the two required rectangular image-transfer function matrices

$\boldsymbol{S}_2$ and $\boldsymbol{S}_3$:

$$Z_1 = (I_n - S_2 \cdot S_3)^{-1} \cdot (I_n + S_2 \cdot S_3) \cdot Z_{I1} \tag{21}$$

$$Z_2 = 2(I_n - S_2 \cdot S_3)^{-1} \cdot S_2 \cdot Z_{I2} \tag{22}$$

$$Z_3 = 2(I_N - S_3 \cdot S_2)^{-1} \cdot S_3 \cdot Z_{I1} \tag{23}$$

$$Z_4 = (I_N - S_3 \cdot S_2)^{-1} \cdot (I_N + S_3 \cdot S_2) \cdot Z_{I2} \tag{24}$$

REFERENCES

1. Speciale, R. A., "Advanced design of phased array beam-forming networks," *IEEE Antenna and Propagation Magazine*, Vol. 38, No. 4, 22–34, August 1996.
2. Speciale, R. A., "Synthesis of phased array aperture distributions," *unpublished monograph*, available for downloading from http://home.comcast.net/∼rspeciale/.
3. Speciale, R. A., "Renormalization of the scattering matrix," *Proceedings of the* 17^{th} *ACES Review*, and also available for downloading from: http://home.comcast.net/∼rspeciale/. Monterey, California, 553–561, March 19–23, 2001.
4. Speciale, R. A., "Suppression of reflections and cross-talk," *Proceedings of the* 17^{th} *Annual Review of Progress in Applied Computational Electromagnetics*, and also available for downloading from: http://home.comcast.net/∼rspeciale/. Monterey, California, 562–573, March 19–23, 2001.